Impact of a Titanium Tibial Implant on the Wireless Charging of a Biomedical Knee Sensor

Nikhil Bejrajh
Department of Electrical Engineering
University of Cape Town
Cape Town, South Africa
bjrnik001@myuct.ac.za

Sampath Jayalath
Department of Electrical Engineering
University of Cape Town
Cape Town, South Africa
sampath.jayalath@uct.ac.z

***Abstract*— Wireless Inductive Power Transfer (WIPT) technology is well suited for biomedical devices as it enables non-invasive charging. This lengthens the operating lifespan of biomedical implants and eliminates the need for further surgeries to remove implants to change their batteries. This paper proposes a magnetic coupler to wirelessly charge a Ligament Balance Measuring System (LBMS) for Total Knee Arthroplasty (TKA) and examines the impact of using a titanium tibial (TiT) component as opposed to a full plastic tibial (PT) component in TKA on the inductive power transfer system. A curved structure is used in the magnetic coupler to utilize the geometry of the knee and sensor. The proposed coupler achieves a coupling coefficient of 0.0286, a 0.2°C temperature increase in biomedical implant due to eddy current heating, a maximum magnetic field strength of 8.5A/m, a peak average SAR of 83 mW/kg and theoretical coil-to-coil efficiency of 88.6% with TiT components. However, with a PT component, the coupling coefficient increases marginally to 0.032, the temperature increase in the biomedical implants due to eddy current heating remains the same at 0.2 °C, the maximum magnetic field strength drops to 4.3 A/m, the peak average SAR drops to 51 mW/kg, and theoretical coil-to-coil efficiency increases to 89.7%. Therefore, the performances of the proposed couplers with the PT outperform the coupler with TiT.**

Keywords—inductive wireless power transfer, biomedical implant charging, biomedical implant heating, magnetic field safety

I. Introduction

Total knee arthroplasty (TKA) is a knee reconstruction procedure used to treat knee trauma resulting from a multitude of injuries including but not limited to fractures, deformities, and secondary or post osteoarthritis which accounts for the majority of cases where patients undergo TKA [1]. Despite being a popular operation, revision surgery for failed TKA is on the rise stemming from infection and mechanical loosening [2]. Revision surgery for failed TKA is costly and puts patients through another recovery period after the surgery.

In [3] a ligament balance measuring system (LBMS) in TKA has been developed to measure the balance between the implanted femoral head and tibia component of the TKA. The LBMS aids surgeons in aligning the implant and can monitor the alignment of the implant when in the patient. This will lower revisions resulting from loosening caused by poor implant alignment and can inform patients if their implant is loosening.

The position of the LBMS, as shown in **Fig. 1** makes it unfeasible to remove the device and replace its battery. Therefore, this paper proposes an inductive wireless power transfer (IWPT) technology to charge the LBMS with a focus on coils or coupler design. IWPT enables non-invasive charging of the LBMS, galvanic isolation from the power supply, and high efficiency.

IWPT systems for biomedical implants must follow the required safety standards to ensure safe operation within a patient. Therefore, the IWPT system should be able to charge the sensor without violating the guidelines for exposure to time-varying magnetic fields set out by the International Commission on Non-Ionising Radiation Protection (ICNIRP) in [4]. This includes not exceeding a specific energy absorption rate (SAR) of 4 W/kg and not causing a temperature increase greater than 1°C in the knee implant [4]. Also, the magnetic field strength (H) should be less than 21 A/m [4] [14].

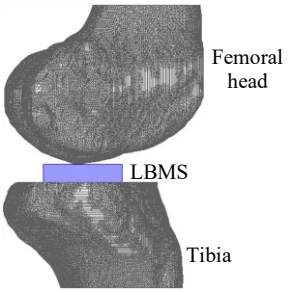

Fig. 1. LBMS device in knee joint

II. Coil Design

A. Simulation Specifications

Before analyzing the performance of the coupler, it is important to define the region in which the coupler will operate, as this will influence the coupling coefficient of the receiver (Rx) and transmitter (Tx) coils. Therefore, 3D models of a femur and tibia were sourced from [5] and [6]. The femoral head and top of the tibia were used from the femur model, as shown in **Fig. 1.** The material properties were set to titanium (Ti) as it is used in TKA [7].

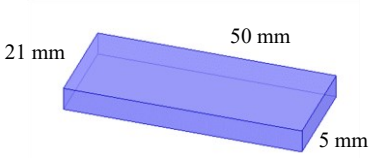

Fig. 2. LBMS in TKA dimensions

However, this option does not apply to all arthroplasties. Therefore, the tibial component material is assigned to Ti, and a comparison simulation with the tibial component material set as plastic is also run. These two simulations will be compared to each other to determine the impact of an all-metal tibial component. The dimensions of the LBMS are shown in **Fig. 2**, and it is modelled out of HDPE. The electrical specifications of the LBMS are outlined in **Table I**.

B. Coil Structure

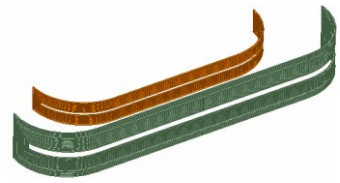

Fig. 3. Coil structure of the proposed inductive coupler (Receiver in orange and transmitter in green).

The coil structure used for the Rx and Tx coil is shown in **Fig. 3**. The Rx is embedded within the LBMS, and the Tx will be positioned outside of the patient on the surface of their knee. **Fig. 4** shows the coupler with the knee implant and LBMS.

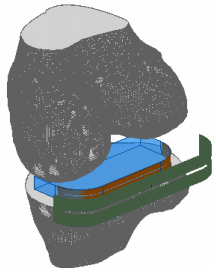

Fig. 4. Coil structure of the proposed inductive coupler.

The Tx and Rx coils are wound with 0.2mm thick wire and have a 0.1 mm coil separation. The Tx has 15 turns and is 70 mm long, while the Rx has 8 turns, and is 50 mm long. This structure couples perpendicular to the patient's leg, which aims to avoid the Ti components blocking the magnetic field from the coupler. When charging the Tx is placed against the knee below the patella which enables easy charging of the LBMS.

C. Compensation Topology

Biomedical implants with a larger size are not readily accepted by the body, resulting in much longer healing times and reduced patient comfort [11]. Therefore, one of the main considerations when choosing a compensation topology was the size and number of components used. As such, the main considerations for compensating the coupler are series-series (SS) and series-parallel (SP) topologies. Additionally, SP compensation has a higher efficiency than SS compensation when Tx and Rx coils differ in size [12]. Although, SS compensation has a lower current in the resonant loop than SP compensation [10]. Increasing the inductance of the Tx and Rx coils allays the concerns of strong magnetic fields resulting from a higher current by reducing the current in the resonant loop. For the above reasons, SP compensation is chosen as the compensation topology for the proposed coupler.

III. System Parameters

The system parameters of the IPT system are outlined in **Table I**. The following equations (1) to (11) detail how the system parameters were calculated [13]:

$$C_{Tx} = \frac{1}{\omega^2 L_{Tx}(1-k^2)} \quad (1)$$

$$C_{Rx} = \frac{1}{\omega^2 L_{Rx}} \quad (2)$$

The approximate AC equivalent resistance of the load is:

$$R_{LAC} = \frac{\pi^2 R_{LDC}}{8} \quad (3)$$

The peak load voltage and peak load current are calculated in (4) and (5) as follows:

$$V_{Lpeak} = \frac{\pi V_{DC}}{2} \quad (4)$$

$$I_{Lpeak} = \frac{4 I_{DC}}{\pi} \quad (5)$$

The peak current for the secondary coil is calculated below:

$$I_{2peak} = \sqrt{I_{Lpeak}^2 + \frac{V_{Lpeak}^2}{(\frac{1}{\omega C_{Rx}})^2}} \quad (6)$$

The source voltage and current for the Tx are calculated below:

$$V_{Speak} = V_{Lpeak}(\frac{M}{L_{Rx}}) \quad (7)$$

$$Z_{Sp} = R_{LAC}(\frac{M}{L_{Rx}})^2 \quad (8)$$

$$I_{1peak} = \frac{V_{Speak}}{Z_{Sp}} \quad (9)$$

$$\eta = \frac{P_O}{P_{IN}} \quad (10)$$

$$P_O = P_{IN} - P_{WINDING} \quad (11)$$

IV. Results

Two simulation setups were used to determine the impact of a full metal tibial component. Setup A includes the Ti femoral head as well as the TiT component. Setup B only includes the Ti femoral head and uses a PT component.

TABLE I. SYSTEM PARAMETERS

Parameter	Value with TiT	Value without TiT
Sensor power rating	139 µW	139 µW
Sensor voltage rating	3.70V	3.70V
Sensor current rating	37.6 µA	37.6 µA
DC load resistance	98.5 kΩ	98.5 kΩ
Frequency (f_0)	10 MHz	10 MHZ
Primary Self-Inductance	12.1 µH	10.9 µH
Secondary Self-Inductance	2.44 µH	2.46 µH
Mutual Inductance	155 nH	166 nH
Primary Compensation Capacitor (C1)	21.0 pF	23.3 pF
Secondary Compensation Capacitor (C2)	103 pF	103 pF
Primary Peak Current (I_{1peak})	37.6 mA	37.6 mA
Secondary Peak Current (I_{2peak})	47.9 µA	47.9µA
Coupling Coefficient (k)	0.0286	0.0320
Tx Coil Resistance (R1)	1.12 Ω	1.07 Ω
Rx Coil Resistance (R2)	439 mΩ	437 mΩ
AC Equivalent Load Resistance (R_{LAC})	121.5 kΩ	121.5 k Ω

A. Magnetic Field Analysis

Setup A and setup B were simulated in ANSYS Maxwell to determine the magnetic field strength (H) that both setups produced. **Fig. 5** shows the H magnitude that was absorbed by the Ti implants resulting from setup A. **Fig. 6** shows the H magnitude absorbed by the Ti femoral head resulting from setup B. Both couplers are safely within the ICNIRP limit of 21 A/m. It is interesting to note that setup A has a peak magnetic field strength of 8.4683 A/m and setup B has a peak magnetic field strength of 4.29 A/m. Demonstrating that the TiT component increases the magnetic field strength of the

coupler. This results from the TiT component reducing the inductance of the Rx coil and mutual inductance.

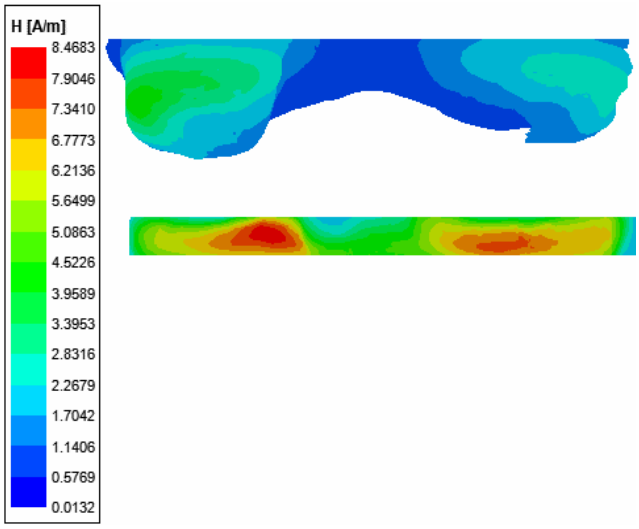

Fig. 5. Magnetic field strength magnitude absorbed by Ti implants with setup A.

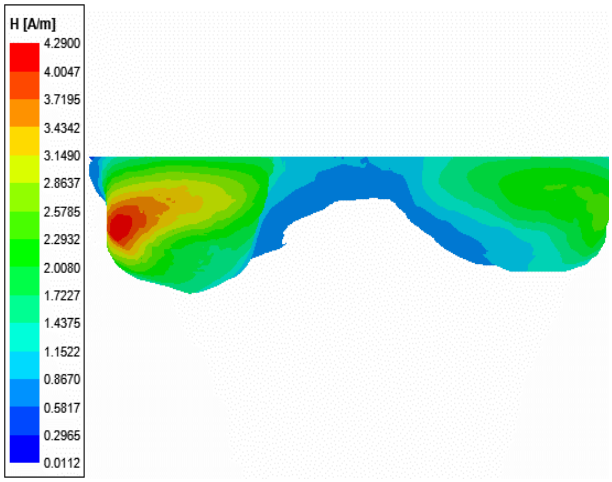

Fig. 6. Magnetic field strength magnitude absorbed by femoral head with setup B (without TiT component).

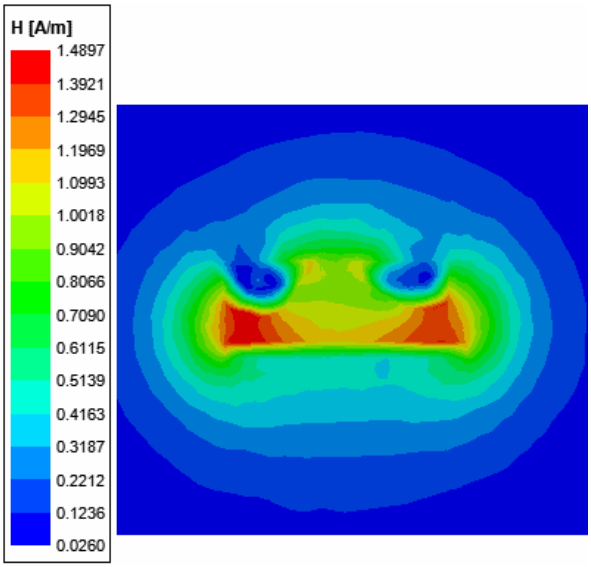

Fig. 7. Magnetic field strength magnitude for setup A.

Fig. 7 illustrates the H magnitude produced by setup A and **Fig. 8** demonstrates the H magnitude produced by setup B.

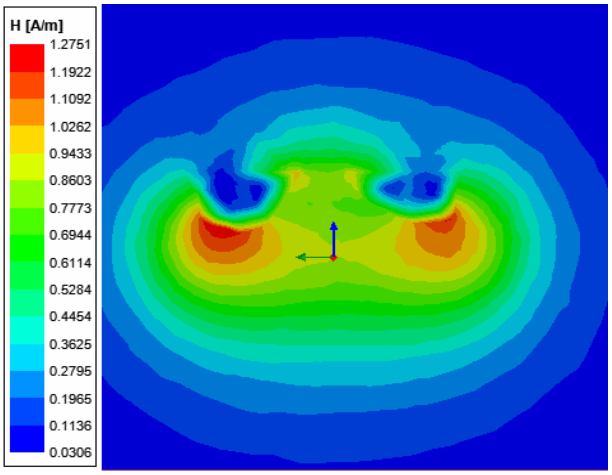

Fig. 8. Magnetic field strength magnitude for setup B.

Setup A produces a higher H magnitude than setup B, 1.4897 A/m compared to 1.2751 A/m. However, both couplers are still well within the limit set out by the ICNIRP of 21 A/m.

B. Temperature Analysis

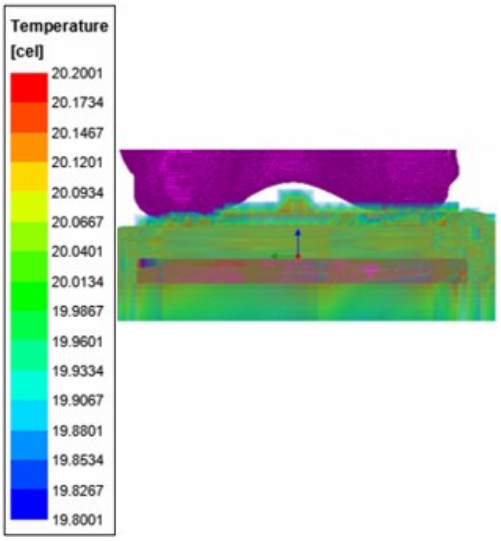

Fig. 9. Temperature of the femoral head and tibial component with setup A.

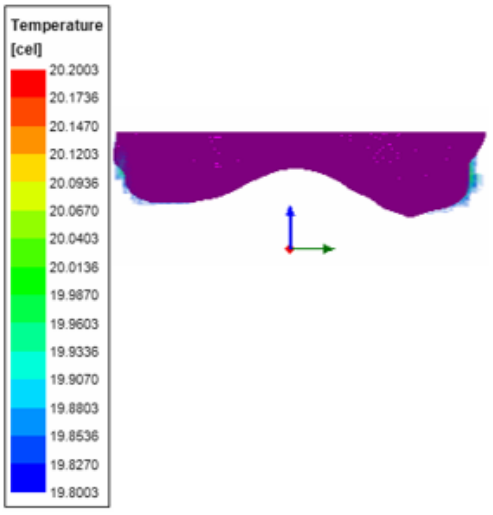

Fig. 10. Temperature of the femoral head for setup B.

ANSYS Icepak was used to simulate setup A and setup B to determine the effect of eddy current heating in the Ti

femoral head and TiT components. The initial temperature of both simulations was set to 20℃.

Fig. 9 and **Fig. 10** show the increase in temperatures of the Ti implants with and without the TiT component because of induced eddy currents in the Ti implants. It is important for the maximum temperature of the Ti implants to be less than 1℃ to meet the guideline set out by the ICNIRP on the temperature rise of a biomedical implant.

In **Fig. 9** and **Fig. 10** the maximum temperature increase in the Ti implants due to eddy current heating is 0.2℃ for setup A and setup B.

C. SAR Analysis

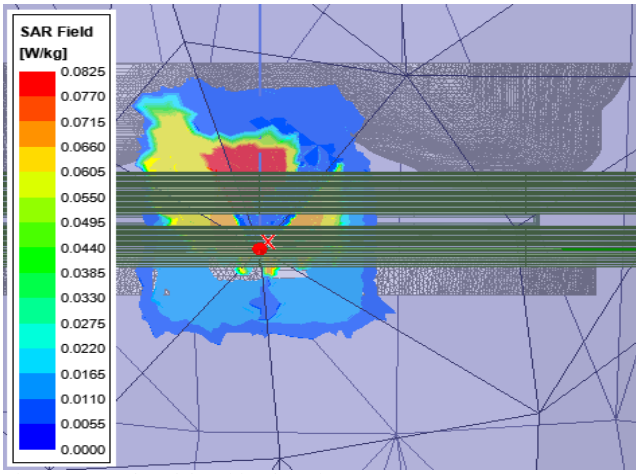

Fig. 11. SAR plot of the Ti implants in setup A.

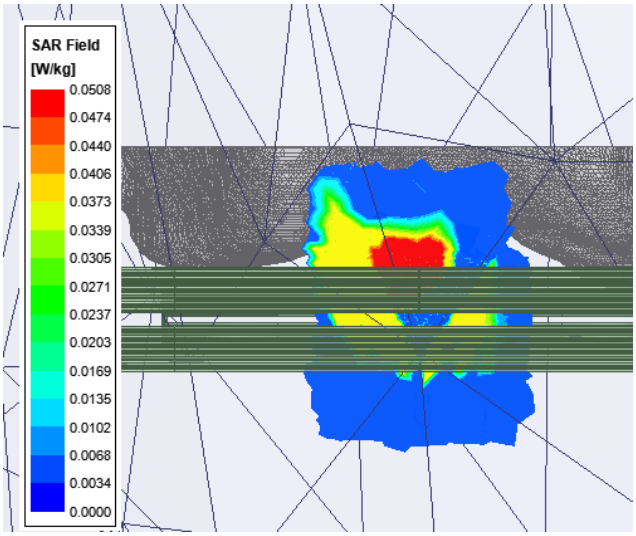

Fig. 12. SAR plot of the Ti implants in setup B.

The peak average SAR analysis of setup A and setup B was carried out in ANSYS HFSS. The SAR plots are displayed in **Fig. 11** and **Fig. 12** for setup A and setup B. The peak average SAR for A is 83 mW/kg and for B the peak average SAR is 51 mW/kg averaged over 1g of tissue. The addition of the TiT causes an increase in the peak average SAR because the metal implants reduce/reflect the electromagnetic fields that strike them onto a smaller region which increases the power absorption in tissue around the implants [15].

D. Efficiency

Using (10) and (11) the theoretical coil-to-coil efficiencies of setup A and setup B are calculated as 88.6% and 89.7%.

E. Misalignment analysis

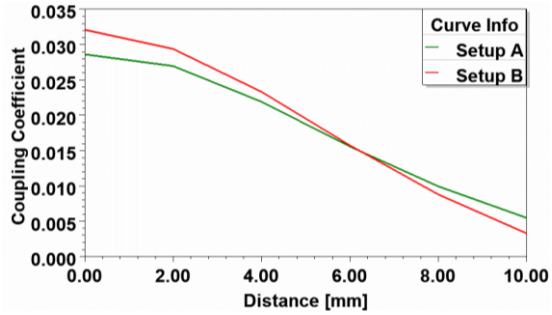

Fig. 13. Misalignment analysis of setup A and B by shifting the transmitter coil down the -z axis.

The misalignment behavior of setups A and B is shown in Fig. 13. The Tx coil is shifted along the -z-axis from 0mm to 10mm. This results in a change of the coupling coefficient from 0.0286 to 0.0055 for setup A. For setup B the coupling coefficient varies from 0.032 to 0.0033 as the Tx is shifted along the -z-axis from 0mm to 10mm.

F. Comparison between setup A and setup B

From the above results, it is evident that the TiT component reduces the mutual inductance and the inductance of the Rx coil. This in turn reduces the coupling coefficient of the magnetic coupler which causes a higher H field in the Ti implants, 8.4683 A/m compared to 4.29 A/m. This results in a higher peak average SAR of 83 mW/kg in setup A when compared to the 51 mW/kg in setup B. Additionally, setup A has a lower drop-off in coupling compared to setup B, 0.0055 compared to 0.0033 at a 10 mm misalignment. This is attributed to the TiT component blocking some of the magnetic fields which would otherwise flow through the Rx coil. Therefore, the coupler with the PT outperforms the coupler with TiT.

V. Future Work and Conclusion

This paper analyzed the impact of a TiT component on the charging of an LBMS in a TKA implant. An IWPT system was designed, and it met the power requirement of 139 µW for the LBMS implant in both setups A and B. Both setups A and B are under the ICNIRP H limit of 21 A/m at 8.4683 A/m and 4.29 A/m respectively. The analysis of Ti implant heating due to eddy currents revealed that setup A and setup B met the ICNIRP standards by having a temperature increase of less than 1 ºC at 0.2 ºC for setups A and B, due to eddy current heating of the implants. The peak average SAR analysis showed that both setup A and setup B are within the ICNIRP limit of 4 W/kg at 83 mW/kg and 51mW/kg. These results reveal that a TiT component will reduce the inductance of the Rx coil and the mutual inductance of the coupler. This in turn causes a greater H field strength, implant heating due to eddy currents, and a higher peak average SAR value. Therefore, a full PT component is preferred but not enforced when implementing an IWPT charging system for a biomedical knee implant sensor.

Future work for this design will involve developing a more realistic phantom with multiple layers representing skin, bone, fat and the ligaments in the knee. Additionally, the bioheat equation will be used to determine the impact of heat transfer to the Ti implants as a result of tissue heating from

the coupler. The bioheat equation considers several factors including blood perfusion, heat conduction between tissue and blood flow in addition to the external heating due to the electromagnetic field produced by the coupler.

VI. Acknowledgements

Intensive computations were performed using facilities provided by the University of Cape Town's High Performance Computing team (hpc.uct.ac.za).

VII. References

[1] J. Manrique, M. R. Rasouli, C. Restrepo, M. G. Maltenfort, J. Beri, J. Oliver, R. Patel, J. Parvizi, "Total Knee Arthroplasty in Patients with Retention of Prior Hardware Material: What is the Outcome?," The Archives of Bone and Joint Surgery, pp. 23-26, January 2018.

[2] R. E. Delanois, J. B. Mistry, C. U. Gwam, N. S. Mohamed, U. S. Choksi, M. A. Mont, " Current Epidemiology of Revision Total Knee Arthroplasty in the United Sates," The Journal of Arthroplasty, vol. 32, no. 9, pp. 2663-2668, 2017.

[3] M. Liu, H. Chen, X. Zhang, C. Zhang, H. Jiang and Z. Wang, "Low-power SoC design for Ligament Balance Measuring System in Total Knee Arthroplasty," 2011 Annual International Conference of the IEEE Engineering in Medicine and Biology Society, Boston, MA, USA, 2011, pp. 5860-5863.

[4] International Commission on Non-Ionizing Radiation Protection (ICNIRP), "Guidelines for limiting exposure to time-varying electric, magnetic, and electromagnetic fields (up to 300 GHz). International Commission on Non-Ionizing Radiation Protection.," Health physics, vol. 74, no. 4, pp. 494-522, Arpil 1998.

[5] My-Segmenter, "Tibia right_human skeleton," National Institute of Health, 17-Feb-2022. [Online]. Available: https://3dprint.nih.gov /discover/3dpx-016824. [Accessed: 09-Feb-2023]

[6] SquareL, "Human Femur," National Institute of Health, 17-Feb-2022. [Online]. Available: https://3dprint.nih.gov/discover/ 3DPX-000168. [Accessed: 09-Feb-2023]

[7] S. H. Ajwani, C. P. Charalambous, "Availability of Total Knee Arthroplasty Implants for Metal Hypersensitivity Patients,' Knee Surgery and Related Research, vol. 28, no. 4, pp. 312-318.

[8] T. Cheng, G. Zhang, X. Zhang, "Metal-backed versus all-polyethylene tibial components in primary total knee arthroplasty," Acta Orthopaedia, vol 82, no. 5, pp. 589-595, October 2011.

[9] T. J. Gioe, A. V. Maheshwari, " The all-polyethylene tibial component in primary total knee arthroplasty," The Journal of Bone and Joint Surgery American Volume, vol. 92, no. 2, pp. 478-487, February 2010.

[10] E. Gati, S. Kokosis, N. Patsourakis, and S. Manias, "Comparison of Series Compensation Topologies for Inductive Chargers of Biomedical Implantable Devices," Electronics, vol. 9, no. 1, p. 8, Dec. 2019.

[11] Davis, R., Singh, A., Jackson, M.J. et al, "A comprehensive review on metallic implant biomaterials and their subtractive manufacturing," The International Journal of Advanced Manufacturing Technologies, vol. 120, pp. 1473–1530, 23 February 2022.

[12] M. Rehman, P. Nallagownden, Z. Baharudin, "Efficiency investigation of SS and SP compensation topologies for wireless power transfer," International Journal of Power Electronics and Drive Systems (IJPEDS), vol. 10, pp. 2157, 1 December 2019.

[13] K. Woronowicz, A. Safaee and T. R. Dickson, "Single-Phase Zero Reactive Power Wireless Power Transfer Topologies Based on Boucherot Bridge Circuit Concept," in Canadian Journal of Electrical and Computer Engineering, vol. 38, no. 4, pp. 323-337, Fall 2015.

[14] I. A. Shah, A. Basir, Y. Cho and H. Yoo, "Safety Analysis of Medical Implants in the Human Head Exposed to a Wireless Power Transfer System," in IEEE Transactions on Electromagnetic Compatibility, vol 64, no. 3, pp. 640-649, June 2022.

[15] D. Bhargava,P. Rattanadecho, T. Wessapan, "The Effect of Metal Objects on the SAR and Temperature Increase in the Human Head," Case Studies in Thermal Engineering, vol. 22, pp. 100789, 2020.